



## **Inactivation of TIF1gamma cooperates with Kras to induce cystic tumors of the pancreas.**

David F. Vincent, Kai-Ping Yan, Isabelle Treilleux, Fabien Gay, Vanessa Arfi, Bastien Kaniewsky, Julien C. Marie, Florian Lepinasse, Sylvie Martel, Sophie Goddard-Leon, et al.

### **► To cite this version:**

David F. Vincent, Kai-Ping Yan, Isabelle Treilleux, Fabien Gay, Vanessa Arfi, et al.. Inactivation of TIF1gamma cooperates with Kras to induce cystic tumors of the pancreas.. PLoS Genetics, 2009, 5 (7), pp.e1000575. 10.1371/journal.pgen.1000575 . inserm-00420083

**HAL Id: inserm-00420083**

**<https://www.hal.inserm.fr/inserm-00420083>**

Submitted on 29 Sep 2009

**HAL** is a multi-disciplinary open access archive for the deposit and dissemination of scientific research documents, whether they are published or not. The documents may come from teaching and research institutions in France or abroad, or from public or private research centers.

L'archive ouverte pluridisciplinaire **HAL**, est destinée au dépôt et à la diffusion de documents scientifiques de niveau recherche, publiés ou non, émanant des établissements d'enseignement et de recherche français ou étrangers, des laboratoires publics ou privés.

# Inactivation of TIF1 $\gamma$ Cooperates with Kras<sup>G12D</sup> to Induce Cystic Tumors of the Pancreas

David F. Vincent<sup>1,2,3,5\*</sup>, Kai-Ping Yan<sup>4\*</sup>, Isabelle Treilleux<sup>5</sup>, Fabien Gay<sup>6</sup>, Vanessa Arfi<sup>1,2,3,5</sup>, Bastien Kaniewsky<sup>1,2,3,5</sup>, Julien C. Marie<sup>7</sup>, Florian Lepinasse<sup>2,6,8</sup>, Sylvie Martel<sup>1,3,5</sup>, Sophie Goddard-Leon<sup>5</sup>, Juan L. Iovanna<sup>9</sup>, Pierre Dubus<sup>10</sup>, Stéphane Garcia<sup>9</sup>, Alain Puisieux<sup>1,2,5</sup>, Ruth Rimokh<sup>1,2</sup>, Nabeel Bardeesy<sup>11</sup>, Jean-Yves Scoazec<sup>2,6,8</sup>, Régine Losson<sup>4</sup>, Laurent Bartholin<sup>1,2,3,5\*</sup>

**1** INSERM, U590, IFR62, Lyon, France, **2** Univ Lyon, Lyon, France, **3** INSERM "Avenir" group, Lyon, France, **4** IGBMC, Strasbourg, Illkirch-Cedex, France, **5** Centre Léon Bérard, Lyon, France, **6** INSERM, U865, Faculté Laennec, Lyon, France, **7** INSERM, U758, Lyon, France, **8** Hospices Civils de Lyon, Hôpital Edouard Herriot, Lyon, France, **9** INSERM, U624, Marseille, France, **10** EA 2406, Univ Bordeaux, France, **11** Massachusetts General Hospital Cancer Center, Harvard Medical School, Boston, Massachusetts, United States of America

## Abstract

Inactivation of the Transforming Growth Factor Beta (TGF $\beta$ ) tumor suppressor pathway contributes to the progression of Pancreatic Ductal AdenoCarcinoma (PDAC) since it is inactivated in virtually all cases of this malignancy. Genetic lesions inactivating this pathway contribute to pancreatic tumor progression in mouse models. Transcriptional Intermediary Factor 1 gamma (TIF1 $\gamma$ ) has recently been proposed to be involved in TGF $\beta$  signaling, functioning as either a positive or negative regulator of the pathway. Here, we addressed the role of TIF1 $\gamma$  in pancreatic carcinogenesis. Using conditional Tif1 $\gamma$  knockout mice (Tif1 $\gamma^{lox/lox}$ ), we selectively abrogated Tif1 $\gamma$  expression in the pancreas of Pdx1-Cre;Tif1 $\gamma^{lox/lox}$  mice. We also generated Pdx1-Cre;LSL-Kras<sup>G12D</sup>;Tif1 $\gamma^{lox/lox}$  mice to address the effect of Tif1 $\gamma$  loss-of-function in precancerous lesions induced by oncogenic Kras<sup>G12D</sup>. Finally, we analyzed TIF1 $\gamma$  expression in human pancreatic tumors. In our mouse model, we showed that Tif1 $\gamma$  was dispensable for normal pancreatic development but cooperated with Kras activation to induce pancreatic tumors reminiscent of human Intraductal Papillary Mucinous Neoplasms (IPMNs). Interestingly, these cystic lesions resemble those observed in Pdx1-Cre;LSL-Kras<sup>G12D</sup>;Smad4<sup>lox/lox</sup> mice described by others. However, distinctive characteristics, such as the systematic presence of endocrine pseudo-islets within the papillary projections, suggest that SMAD4 and TIF1 $\gamma$  don't have strictly redundant functions. Finally, we report that TIF1 $\gamma$  expression is markedly down-regulated in human pancreatic tumors by quantitative RT-PCR and immunohistochemistry supporting the relevance of these findings to human malignancy. This study suggests that TIF1 $\gamma$  is critical for tumor suppression in the pancreas, brings new insight into the genetics of pancreatic cancer, and constitutes a promising model to decipher the respective roles of SMAD4 and TIF1 $\gamma$  in the multifaceted functions of TGF $\beta$  in carcinogenesis and development.

**Citation:** Vincent DF, Yan K-P, Treilleux I, Gay F, Arfi V, et al. (2009) Inactivation of TIF1 $\gamma$  Cooperates with Kras<sup>G12D</sup> to Induce Cystic Tumors of the Pancreas. PLoS Genet 5(7): e1000575. doi:10.1371/journal.pgen.1000575

**Editor:** Bruce E. Clurman, Fred Hutchinson Cancer Research Center, United States of America

**Received:** March 16, 2009; **Accepted:** June 24, 2009; **Published:** July 24, 2009

**Copyright:** © 2009 Vincent et al. This is an open-access article distributed under the terms of the Creative Commons Attribution License, which permits unrestricted use, distribution, and reproduction in any medium, provided the original author and source are credited.

**Funding:** This work was supported by grants from, ARC 3891 (LB), INSERM "Avenir" program (LB), INCA "libre" (RR/LB, JYS, and JCM), INCA "plateforme" (LB and JCM), and Ligue Contre le Cancer (LB). DFV is a MENRT doctoral fellow. The funders had no role in study design, data collection and analysis, decision to publish, or preparation of the manuscript.

**Competing Interests:** The authors have declared that no competing interests exist.

\* E-mail: bartholi@lyon.fnclcc.fr

† Current address: The Wistar Institute, Philadelphia, Pennsylvania, United States of America

‡ These authors contributed equally to this work.

## Introduction

Pancreatic Ductal AdenoCarcinoma (PDAC), characterized by a ductal cell-type differentiation pattern, is the most common type of pancreatic cancer, accounting for more than 85% of pancreatic neoplasms. PDAC is the fourth leading cause of cancer-related mortality and carries an overall 5-year-survival rate of less than 5% [1]. The poor outcome of these patients is due to late diagnosis and resistance to current therapies. PDAC appears to arise from precursor lesions known as Pancreatic Intraepithelial Neoplasia (PanINs) or from two types of cystic tumors: Mucinous Cystic Neoplasms (MCNs) and Intraductal Papillary Mucinous Neoplasms (IPMNs) [2]. Mucinous cystic neoplasms are cysts lined by mucin-producing epithelial cells usually associated with an

ovarian-type of stroma. These cysts do not communicate with the larger pancreatic ducts. IPMNs form intraductal papillary projections replacing the normal duct epithelium, secrete mucin, and communicate with ducts. IPMNs are currently classified according to their pattern of apparent histological differentiation into three main subtypes: intestinal (with the neoplastic epithelium resembling the intestinal epithelium), the most frequent, pancreatobiliary and gastric [3].

Recurrent genetic alterations have been identified in human PDAC [4,5]. Sporadic cases, which represent the vast majority of PDAC, are associated with activation of the *KRAS* oncogene (>90% of cases) and inactivation of the *INK4A/ARF* (>80% of cases), *TP53* (>50% of cases) and *SMAD4/DPC4* (>50% of cases) tumor suppressors. Inherited pancreatic cancers represent approx-

## Author Summary

Inactivation of the TGF $\beta$  tumor suppressor pathway contributes to the progression of Pancreatic Ductal Adenocarcinoma (PDAC), a devastating malignancy. Transcriptional Intermediary Factor 1 $\gamma$  (TIF1 $\gamma$ ) has recently been proposed to be involved in TGF $\beta$  signaling, a pathway inactivated in virtually all cases of this malignancy. To address the role of TIF1 $\gamma$  in pancreatic carcinogenesis, we used conditional *Tif1 $\gamma$*  knockout mice. In a genetic background expressing a constitutively active mutation of *KRAS* oncogene (*Kras*<sup>G12D</sup>) recurrently found in patients with PDAC, *Tif1 $\gamma$*  inactivation induces pancreatic precancerous lesions resembling those observed in the absence of *Smad4*, a key player involved TGF $\beta$  signal transduction. This observation strengthens the notion that TIF1 $\gamma$  plays an active role in TGF $\beta$  signaling. Interestingly, we also found that TIF1 $\gamma$  expression was markedly down-regulated in human pancreatic tumors supporting the relevance of our findings to human malignancy. Characterization of new players involved in the outbreak of early pancreatic lesions that will eventually evolve into invasive pancreatic cancer is crucial to detect the disease earlier and eventually develop new therapeutic drugs.

imately 5–10% of all pancreatic cancers. In a high proportion of familial pancreatic cancers, the genetic alterations causing the disease are still unknown. However, several germinal mutations associated with complex familial syndromes have been shown to significantly increase the risk of developing pancreatic cancer (*BRCA2*, *INK4A*, *STK11/LKB1*, *PRSS1*, *hMLH1* and *hMSH2*) [1,6].

In the last five years, a series of genetically engineered mouse models of PDAC have been developed based on these signature gene mutations [7]. For instance, expression of a constitutively active *Kras* mutant protein (*Kras*<sup>G12D</sup> or *Kras*<sup>G12V</sup>) induces PanINs that eventually progress towards PDAC [8,9,10]. *Kras* activated mutants act in concert with inactivation of the p53 [11], *Ink4A/Arf* [12,13], and *TBR1* [14] tumor suppressors to accelerate development of PDAC. These models and others [15–19] support the concept that progression towards invasive PDAC involves emergence from different precancerous lesions (PanINs, MCNs and IPMNs) depending on the associated genetic alterations.

The TGF $\beta$  pathway appears to be of particular importance to PDAC tumor suppression, since it is inactivated in virtually all cases of this malignancy [20], and since genetic lesions inactivating the pathway—inactivation of *Smad4* or *TBR1* and over-expression of inhibitory *Smad7*—contribute to pancreatic tumor progression in mouse models [14,21–24]. Transforming growth factor beta (TGF $\beta$ ) is a secreted polypeptide belonging to a wide family of cytokines and growth factors including TGF $\beta$ s, Bone Morphogenetic Proteins (BMPs) and activins [25,26]. Upon binding to its receptors, TGF $\beta$  triggers phosphorylation of the SMAD2 and SMAD3 transcription factors. Phosphorylated SMAD2 and SMAD3 then interact with SMAD4. The SMAD2/3/4 complex accumulates within the nucleus, binds to DNA and activates the transcription of target genes leading to proliferative arrest or apoptosis of epithelial cells.

Transcriptional Intermediary Factor 1 gamma (also named TIF1 $\gamma$ /TRIM33/RF37/PTC7/Ectoderm) [27,28] appears to contribute to TGF $\beta$  signaling, although its precise functional role is not clear. Some data point toward TIF1 $\gamma$  as a negative regulator of the pathway through its capacity to mono-ubiquitinate SMAD4 and limit SMAD4 nuclear accumulation [29,30,31]. In contrast,

other studies have suggested that TIF1 $\gamma$  plays an important positive role in transducing TGF $\beta$  signaling through its interaction with SMAD2 and SMAD3 [32].

Here we wished to determine whether TIF1 $\gamma$  contributes to tumorigenesis consistent with a function within the TGF $\beta$  signaling pathway. We have focused on pancreatic exocrine tumors based on the prominent role played by TGF $\beta$  signaling in these malignancies. Using a conditional mouse strain, we show for the first time that *Tif1 $\gamma$*  is an important gene whose loss of function cooperates with *Kras*<sup>G12D</sup> activation to induce cystic pancreatic tumors resembling human IPMNs. We also report that *TIF1 $\gamma$*  expression is down-regulated in human PDAC and some types of precursor lesions, supporting the relevance of our mouse model to human malignancy.

## Results/Discussion

To selectively abrogate *Tif1 $\gamma$*  expression in the pancreas, we crossed conditional *Tif1 $\gamma$*  knockout mice [33] with *Pdx1-Cre* mice [34]. *Pdx1* is a gene expressed in the common progenitor to all pancreatic lineages during early embryogenesis, hence *Pdx1-Cre* transgenic mice exhibit recombination of floxed alleles in pancreatic cells from all lineages (endocrine, acinar, centroacinar and ductal cells) [35]. *Pdx1-Cre;Tif1 $\gamma$ <sup>lox/lox</sup>* animals were born at expected ratios and showed normal lifespan without obvious developmental or physiological alterations. Live imaging techniques (Positron Emission Tomography, PET and Magnetic Resonance Imaging, MRI), histological techniques (immunodetection of insulin, glucagon, PPY, chymotrypsin, F4/80, CD3, MPO), metabolic tests (glucose tolerance) did not reveal any significant differences between wild-type and *Pdx1-Cre;Tif1 $\gamma$ <sup>lox/lox</sup>* littermates ( $n > 20$ , between 3 weeks and 2 years of age) (data not shown). As expected, immunohistochemistry experiments showed that Tif1 $\gamma$  was expressed in the nuclei of pancreatic cells in wild-type mice and that this staining was lost in the *Pdx1-Cre;Tif1 $\gamma$ <sup>lox/lox</sup>* pancreas (Figure S1). In all, these observations show that *Tif1 $\gamma$*  is dispensable for normal pancreatic development and function in the mouse.

Activating *KRAS* mutations occur early in human PDAC pathogenesis and give rise to slowly progressing PanINs in mouse models [8,10,12]. We then asked whether *Tif1 $\gamma$*  inactivation could modify the phenotype or latency of the pancreatic lesions induced by *Kras*<sup>G12D</sup>. To that end, we generated *Pdx1-Cre;LSL-Kras*<sup>G12D</sup>; *Tif1 $\gamma$ <sup>lox/lox</sup>* mice ( $n = 12$ , Table S1). All animals looked healthy at the time they were euthanized (the oldest animal was sacrificed at the age of 189 days). Since pancreatic lesions are often asymptomatic, we decided to explore *in vivo* the pancreas of these mutant mice ( $n = 4$ ) by PET and MRI imaging techniques. *Pdx1-Cre;LSL-Kras*<sup>G12D</sup>; *Ink4A/Arf*<sup>lox/lox</sup> mice, which exhibit rapid PDAC progression, were also employed in these studies. Strikingly, MRI imaging performed on *Pdx1-Cre;LSL-Kras*<sup>G12D</sup>; *Tif1 $\gamma$ <sup>lox/lox</sup>* animals revealed an hypertrophic pancreas with multifocal cystic lesions exhibiting T2 hypersignals visible as early as 7 weeks after birth (T2 weighted scans allow detection of cysts as they are sensitive to water content) (Figure 1B). Such lesions were absent in the pancreas of wild-type and *Pdx1-Cre;LSL-Kras*<sup>G12D</sup> animals (Figure 1A) and were clearly different from those observed in *Pdx1-Cre;LSL-Kras*<sup>G12D</sup>; *Ink4A/Arf*<sup>lox/lox</sup> mice, which harbor solid tumors exhibiting a T1 isosignals (T1 weighed scans allow detection of solid tumors) (Figure 1C). PET imaging did not show significant increased metabolic activity in the abdomen of wild-type (Figure 1D) and *Pdx1-Cre;LSL-Kras*<sup>G12D</sup>; *Tif1 $\gamma$ <sup>lox/lox</sup>* mice (Figure 1E) whereas *Pdx1-Cre;LSL-Kras*<sup>G12D</sup>; *Ink4A/Arf*<sup>lox/lox</sup> mice had abdominal lesions with readily detectable metabolic activity



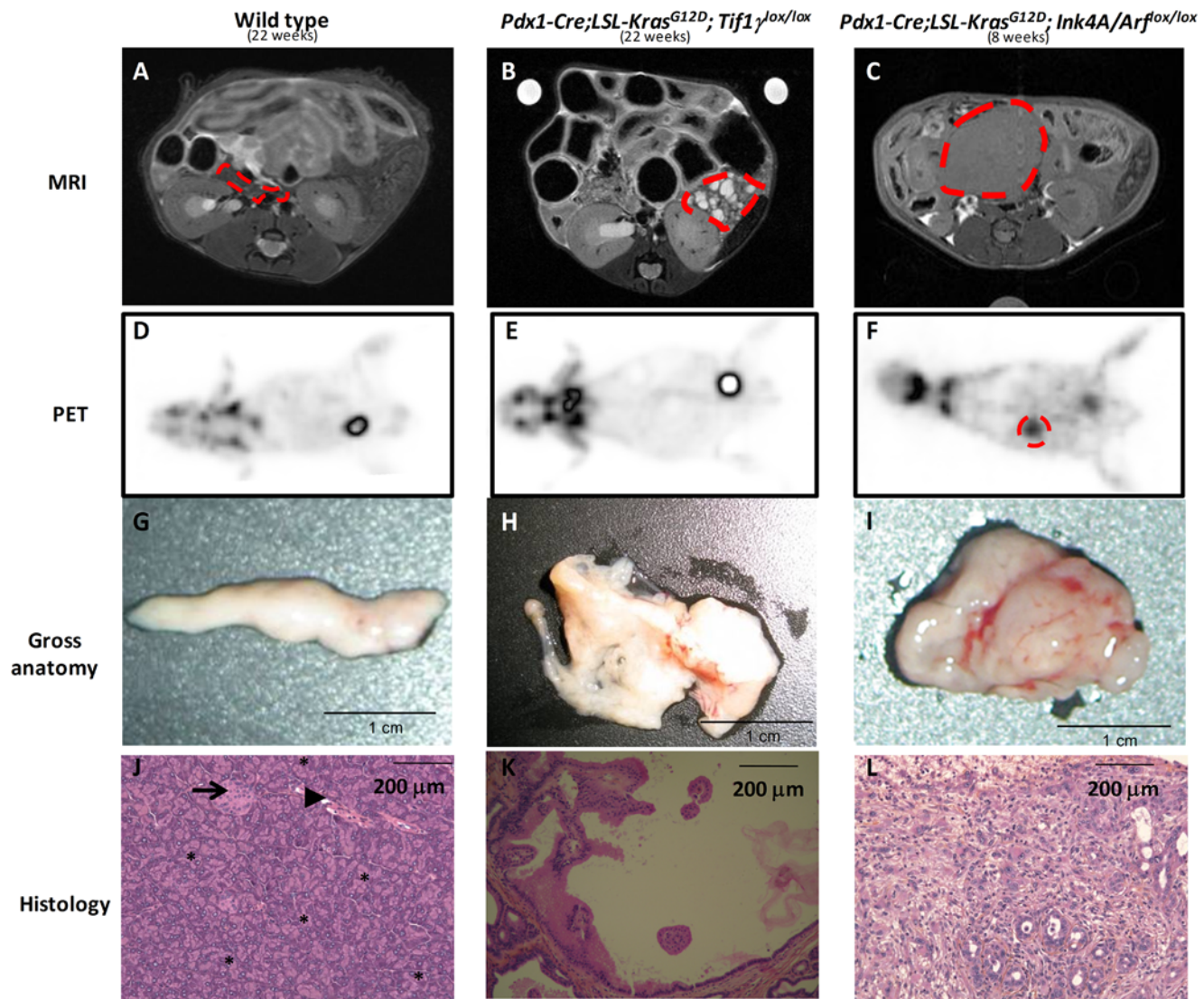


**Figure 1. Homozygous deletion of *Tif1 $\gamma$*  cooperates with activated *Kras*<sup>G12D</sup> mutation to induce cystic tumors of the pancreas.** Magnetic Resonance Imaging (MRI) (A–C). Positron Emission Tomography (PET) (D–F). Gross anatomy of the pancreas after dissection (G–I). Hematoxylin Phloxine Saffron (HPS) staining of pancreas sections (J–L). Acinar tissue (stars), scattered endocrine islets (arrow) and exocrine ducts (arrowhead). When notified, pancreas is circled in red dashed lines. *Pdx1-Cre;LSL-Kras*<sup>G12D</sup>;*Tif1 $\gamma$* <sup>lox/lox</sup> used in this experiment was 154 days old and representative of the 4 mice we analyzed at the age of 18–27 weeks.  
doi:10.1371/journal.pgen.1000575.g001

(Figure 1F). Macroscopic analysis of the *Pdx1-Cre;LSL-Kras*<sup>G12D</sup>;*Tif1 $\gamma$* <sup>lox/lox</sup> pancreas confirmed the presence of numerous cysts affecting the entire organ without macroscopic evidence of invasive carcinoma (Figure 1H and Figure S2) whereas the pancreas of *Pdx1-Cre;LSL-Kras*<sup>G12D</sup>;*Ink4A/Arf*<sup>lox/lox</sup> mice was invaded by a firm and homogeneous mass (Figure 1I) and the pancreas from wild-type or *Pdx1-Cre;LSL-Kras*<sup>G12D</sup> animals had a normal macroscopic appearance (Figure 1G). The size of these cysts observed in the pancreas from *Pdx1-Cre;LSL-Kras*<sup>G12D</sup>;*Tif1 $\gamma$* <sup>lox/lox</sup> was variable and most of them contained papillary projections (Figure 1K). These lesions clearly contrast with the invasive tumors of ductal morphology identified as PDAC in the pancreas of *Pdx1-Cre;LSL-Kras*<sup>G12D</sup>;*Ink4A/Arf*<sup>lox/lox</sup> (Figure 1L). The histological analysis of the 12 *Pdx1-Cre;LSL-Kras*<sup>G12D</sup>;*Tif1 $\gamma$* <sup>lox/lox</sup> animals (Table S1) revealed the presence of cystic lesions in 100% of these mice, such cysts being never observed in *Pdx1-Cre;LSL-Kras*<sup>G12D</sup> or wild type control animals. Quantitative analysis revealed that the area

occupied by the abnormal pancreas exceeded 50% by the age 6 weeks in 6/7 *Pdx1-Cre;LSL-Kras*<sup>G12D</sup>;*Tif1 $\gamma$* <sup>lox/lox</sup> mice whereas it represented less than 20% in 6/6 *Pdx1-Cre;LSL-Kras*<sup>G12D</sup> mice (Table S1). Collectively these data demonstrate that inactivation of *Tif1 $\gamma$*  actively cooperates with activated *Kras*<sup>G12D</sup> to induce cystic tumors of the pancreas.

To carefully compare the pancreatic lesions observed in *Pdx1-Cre;LSL-Kras*<sup>G12D</sup>;*Tif1 $\gamma$* <sup>lox/lox</sup> with the *Pdx1-Cre;LSL-Kras*<sup>G12D</sup> controls, we performed a sequential histological analysis of pancreas from animals (n = 12) euthanized at different ages (Table S1). Contrary to wild-type mice (Figure 2A–2D), *Pdx1-Cre;LSL-Kras*<sup>G12D</sup> mice gradually developed focal PanINs by the age of about 10 weeks (Figure 2E–2H). Strikingly, in *Pdx1-Cre;LSL-Kras*<sup>G12D</sup>;*Tif1 $\gamma$* <sup>lox/lox</sup> pancreas, PanINs, signs of acute inflammation as well as enlarged and dilated ductal structure resembling budding cysts were observed as early as 3 weeks of age (Figure 2I and Figure S3). At later time points, inflammatory tissue and PanINs were mainly

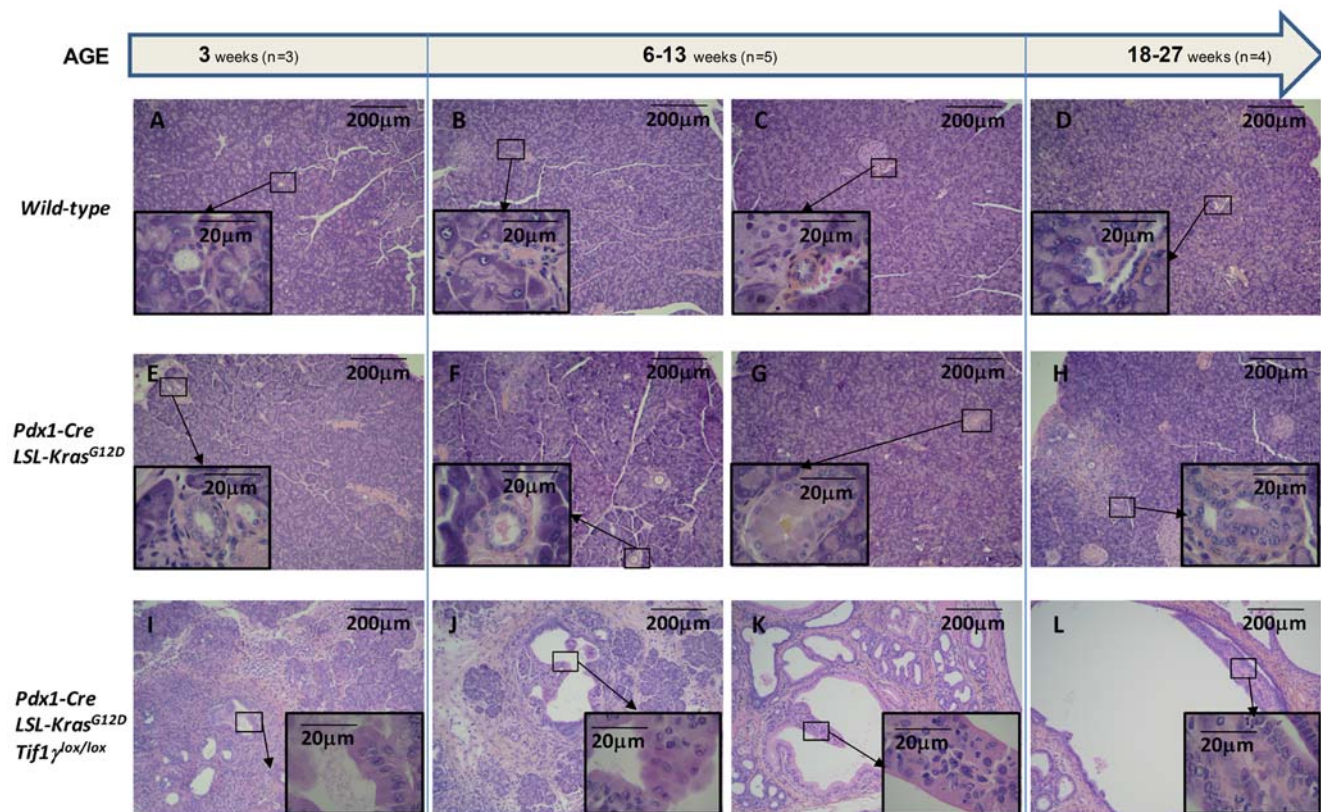


**Figure 2. Inactivation of *Tif1 $\gamma$*  accelerates activated *Kras*<sup>G12D</sup>-mediated pancreatic neoplasia.** Sections of wild-type (A–D), *Pdx1-Cre*;*LSL-Kras*<sup>G12D</sup> (E–H) and *Pdx1-Cre*;*LSL-Kras*<sup>G12D</sup>;*Tif1 $\gamma$* <sup>lox/lox</sup> (I–L) pancreas from mice at different ages were stained with HPS. Number of mice: 3 weeks, n = 3; 6–13 weeks, n = 5; 18–27 weeks, n = 4. Inset pictures: Higher magnification.  
doi:10.1371/journal.pgen.1000575.g002

replaced with cystic lesions becoming more numerous and of larger size (Figure 2J–2L). Microscopic examination revealed that the lining of the cystic structures characteristically found in the pancreas from *Pdx1-Cre*;*LSL-Kras*<sup>G12D</sup>;*Tif1 $\gamma$* <sup>lox/lox</sup> mice was formed by epithelial cells with a cuboidal or cylindrical morphology. These cells formed numerous thick papillary projections in the cyst lumen. The axis of these projections usually contained masses of small monomorphic cells with an endocrine morphology (Insets in Figure 2I–2L).

We performed immunohistochemical studies to characterize the evolving pancreatic lesions in these mice. We observed staining for chymotrypsin and insulin, which decreased with age, indicating a replacement of exocrine and endocrine components, together with abnormal ductal structures in *Pdx1-Cre*;*LSL-Kras*<sup>G12D</sup>;*Tif1 $\gamma$* <sup>lox/lox</sup> mice (Figure 3). There was a notable disappearance of well-organized endocrine islets with age coinciding with the accumulation of endocrine cells within the papillary projections bulging within the lumen of the cysts.

To more precisely identify the nature of these lesions, several lineage markers were explored by immunohistochemistry. We first verified that *Tif1 $\gamma$*  expression was lost in pancreatic ducts from *Pdx1-Cre*;*LSL-Kras*<sup>G12D</sup>;*Tif1 $\gamma$* <sup>lox/lox</sup> mice (Figure 4E) compared to normal observed ducts in wild-type mice (Figure 4A). In the normal pancreas, cytokeratin 19 (CK19) is specifically expressed by ductal cells lining the secretory ducts (Figure 4B). We verified that most of the epithelial cells lining the cystic lesions observed in *Pdx1-Cre*;*LSL-Kras*<sup>G12D</sup>;*Tif1 $\gamma$* <sup>lox/lox</sup> mice were positive for CK19 (Figure 4F); this is consistent with a ductal phenotype for these cells. However, in contrast to the cells lining the normal

secretory ducts (Figure 4C), many cells lining the cysts were mucus-secreting and stained for Alcian blue (Figure 4G). The cells with an endocrine appearance present within the intra-cystic papillary projections were CK19 and Alcian blue negative. There was no evidence of ovarian-type stroma or of invasive or microinvasive carcinoma, even on serial sections, suggesting that these cystic tumors resemble human IPMNs. In all, the cystic lesions observed in *Pdx1-Cre*;*LSL-Kras*<sup>G12D</sup>;*Tif1 $\gamma$* <sup>lox/lox</sup> mice show distinctive characteristics, including the presence of intra-epithelial endocrine pseudo-islets, suggestive of a mixed, endocrine-exocrine, lesion [7].

TIF1 $\gamma$  has recently been proposed to be involved in TGF $\beta$  signaling [29,32]. The resemblance between the cystic lesions (either IPMNs [21,23] or MCNs [22]) observed in *Pdx1-Cre*;*LSL-Kras*<sup>G12D</sup>;*Smad4*<sup>lox/lox</sup> mice, and the cystic lesions we observed in the *Pdx1-Cre*;*LSL-Kras*<sup>G12D</sup>;*Tif1 $\gamma$* <sup>lox/lox</sup> mice, reinforces an active role of TIF1 $\gamma$  in TGF $\beta$  signaling. However, we cannot rule out the possibility that TIF1 $\gamma$  could also be involved in other signaling pathways. Interestingly, we observed that *Smad4* expression was almost undetectable in epithelial cells lining the papillary projections observed in *Pdx1-Cre*;*LSL-Kras*<sup>G12D</sup>;*Tif1 $\gamma$* <sup>lox/lox</sup> mice whereas it was detectable in epithelial cells lining the cysts (Figure 4H) or in normal ducts (Figure 4D). IPMNs observed in *Pdx1-Cre*;*LSL-Kras*<sup>G12D</sup>;*Tif1 $\gamma$* <sup>lox/lox</sup> mice always contain a significant endocrine component, a rare event in IPMNs observed in *Pdx1-Cre*;*LSL-Kras*<sup>G12D</sup>;*Smad4*<sup>lox/lox</sup> mice [21,23]. This observation suggests that TIF1 $\gamma$  and SMAD4 could differentially regulate endocrine versus exocrine differentiation in a context of an activated KRAS oncogenic protein.



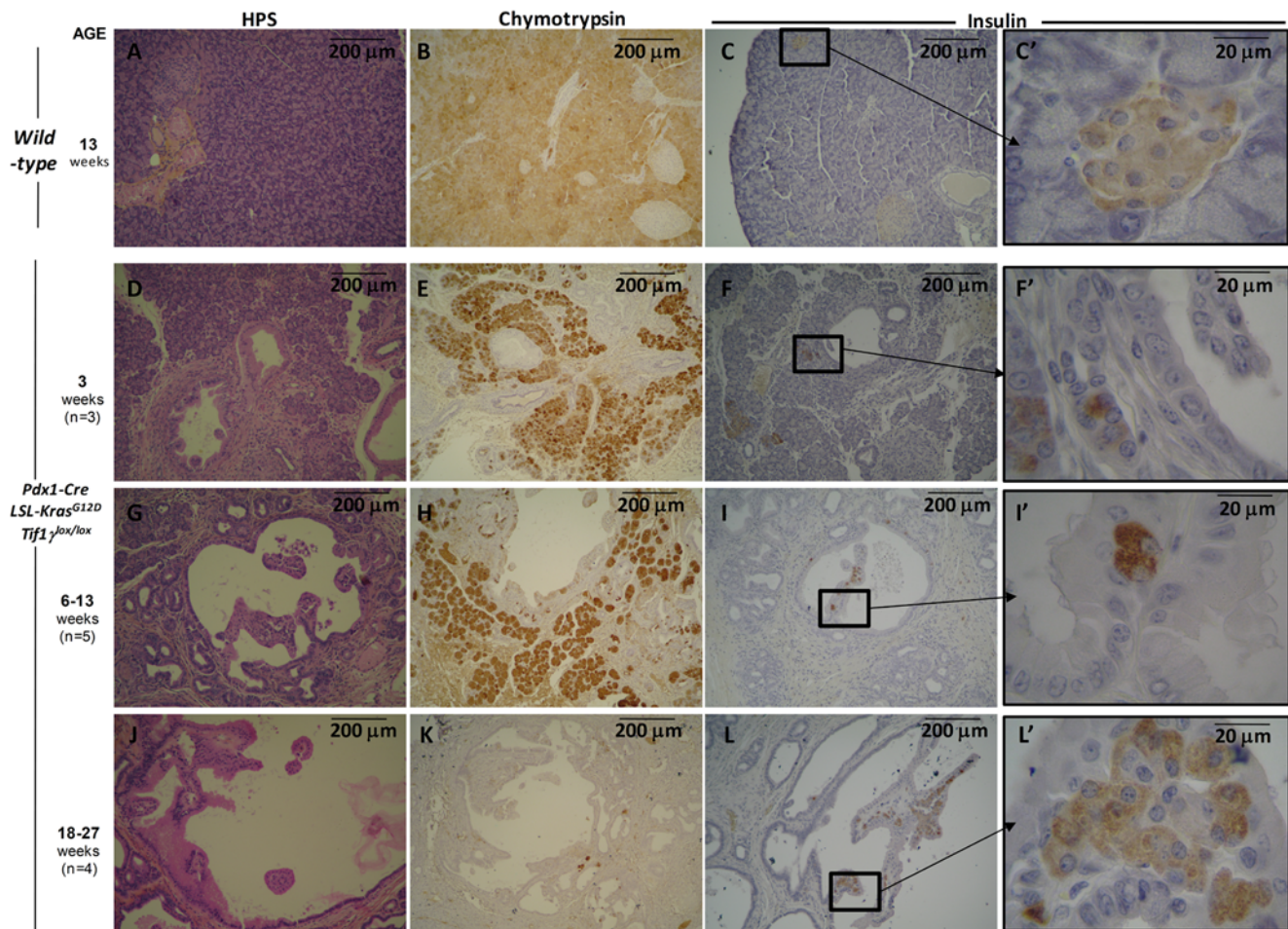


**Figure 3. Endocrine and exocrine compartments destruction in the pancreas of *Pdx1-Cre;LSL-Kras<sup>G12D</sup>;Tif1 $\gamma$ <sup>lox/lox</sup>* mice.** Wild-type (A–C') and *Pdx1-Cre;LSL-Kras<sup>G12D</sup>;Tif1 $\gamma$ <sup>lox/lox</sup>* (D–L') pancreas sections were stained with HPS (A,D,G,J), immuno-revealed either with an anti-chymotrypsin antibody (B,E,H,K) or an anti-insulin antibody (C,F,I,L and C',F',I',L' that represent the boxed region in C,F,I,L at a higher magnification). For *Pdx1-Cre;LSL-Kras<sup>G12D</sup>;Tif1 $\gamma$ <sup>lox/lox</sup>* mice, analysis were performed at different ages. Number of mice: 3 weeks, n = 3; 6–13 weeks, n = 5; 18–27 weeks, n = 4. Boxes: Higher magnification. The pictures show one representative mouse for each group.  
doi:10.1371/journal.pgen.1000575.g003

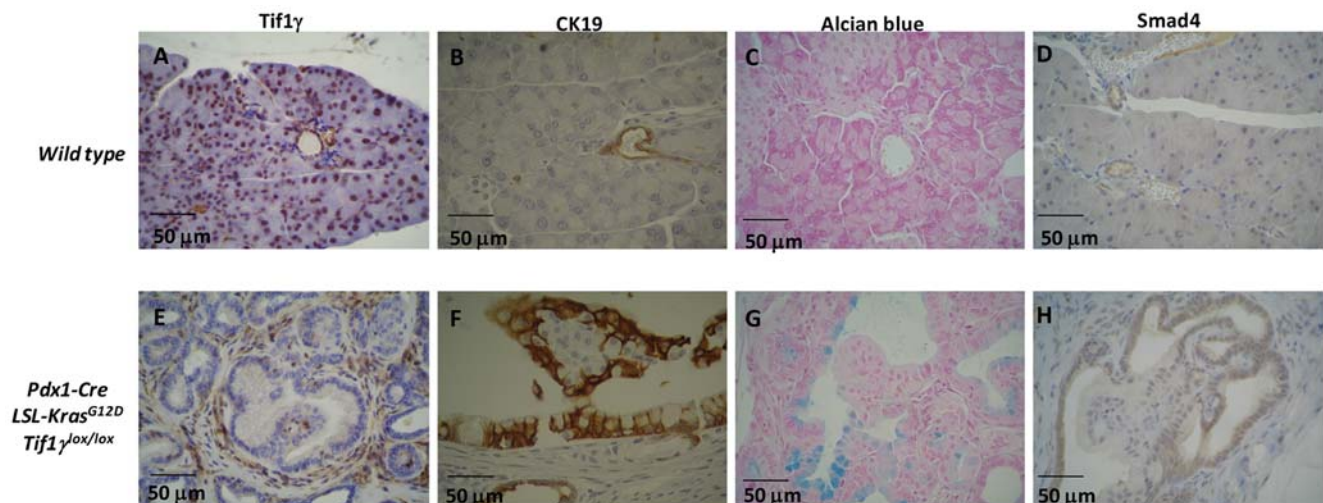


**Figure 4. Immunophenotyping of pancreas cysts observed in *Pdx1-Cre;LSL-Kras<sup>G12D</sup>;Tif1 $\gamma$ <sup>lox/lox</sup>* mice.** Wild-type (A–D) and *Pdx1-Cre;LSL-Kras<sup>G12D</sup>;Tif1 $\gamma$ <sup>lox/lox</sup>* (E–H) pancreas sections were stained to detect glandular cells (CK19), mucus-secreting cells (Alcian Blue), Tif1 $\gamma$  and Smad4. The pictures show one representative mouse at the age of 22 weeks.  
doi:10.1371/journal.pgen.1000575.g004

Based on the prominent cooperation noted between *Kras* activation and *Tif1 $\gamma$*  inactivation in promoting cystic pancreatic tumors in our mouse model, we speculated that *TIF1 $\gamma$*  expression may be down-regulated in human pancreatic tumors. To test this hypothesis, we analyzed by quantitative RT-PCR the expression level of *TIF1 $\gamma$*  and *SMAD4* mRNA in 20 PDAC and 16 peritumoral tissues coming from surgical specimens removed for therapeutic purposes (peritumoral tissues were not available for 4 of these patients). The cellularity of the samples used for molecular analysis was verified histologically. Our results show that *TIF1 $\gamma$*  expression is significantly decreased in the tumors as compared to peritumoral tissues ( $P=0.0054$ ) (Figure 5A). We also compared *TIF1 $\gamma$*  expression levels in each individual tumor along with the peritumoral tissue from the same patient ( $n=16$ ). Our results show that *TIF1 $\gamma$*  expression is significantly down-regulated in most patients and is not up-regulated in any patient (Figure 5B). We next examined *TIF1 $\gamma$*  protein pattern of expression by immunohistochemistry in human pancreatic cancers and their precursors. In peritumoral tissues from PDAC, *TIF1 $\gamma$*  was detected in the majority of the nuclei of acinar, ductal and endocrine cells (Figure 5C). Centroacinar cells are more difficult to identify in routinely stained sections; however, since no epithelial cell population devoid of *TIF1 $\gamma$*  expression has been detected in the normal pancreas, it can be assumed that they also express *TIF1 $\gamma$* . In PDAC (16 cases), *TIF1 $\gamma$*  nuclear expression level was significantly decreased as compared to the peritumoral tissue. In 8 cases, *TIF1 $\gamma$*  expression was heterogeneous, with large numbers of negative cells coexisting with scattered positive cells (Figure 5D). In 2 cases, *TIF1 $\gamma$*  was even undetectable (Figure 5E). In IPMNs (samples from 10 patients, all with the intestinal subtype according to current classifications [3]), almost all neoplastic cells in areas of low grade dysplasia (present in the 10 cases) displayed a weak nuclear positivity whereas in areas of high grade dysplasia (present in the 10 cases), more than 50% of cells were negative for *TIF1 $\gamma$* ; this was especially the case along the papillary projections (Figure 5F). In PanINs (samples from 15 patients, with grade 1 in 12, grade 2 in 10 and grade 3 in 8), the expression of *TIF1 $\gamma$*  was usually retained in grade 1 and 2 lesions (data not shown), but was undetectable in a variable proportion of cells in grade 3 lesions (Figure 5G). In MCNs (8 cases), *TIF1 $\gamma$*  protein was strongly expressed by all neoplastic cells, even in areas of high grade dysplasia and in foci of microinvasive carcinoma (Figure 5H). We showed in the same set of tumors that *SMAD4* expression was also down-regulated in high-grade PanINs, IPMNs and PDAC, while remained highly expressed in MCNs (Figure S4).

None of the *Pdx1-Cre;LSL-Kras<sup>G12D</sup>;Tif1 $\gamma$ <sup>lox/lox</sup>* mice ( $n=4$ ) sacrificed after the age of 13 weeks showed an aggressive cancer developed from IPMNs. This observation is consistent with epidemiological data in humans showing that IPMNs only rarely give rise to aggressive tumors [3]. Interestingly, IPMNs were reported in *Pdx1-Cre;LSL-Kras<sup>G12D</sup>;Smad4<sup>lox/lox</sup>* mice but no PDAC was found by the age of 13 weeks ( $n=8$ ) [21]. Another group observed in *Pdx1-Cre;LSL-Kras<sup>G12D</sup>;Smad4<sup>lox/lox</sup>* a significant proportion of PDAC between 23 and 33 weeks [23]. This suggests that the minimal latency period to see the onset of aggressive tumors may have not been reached in our study or the number of animals studied is too low. We have been in the process of “aging” a cohort of *Pdx1-Cre;LSL-Kras<sup>G12D</sup>;Tif1 $\gamma$ <sup>lox/lox</sup>* mice to address this specific point even if we cannot rule out the possibility that these animals die before developing aggressive tumors because of pancreatic failure due to growing cysts. The molecular mechanism supporting the cooperation between activated *Kras<sup>G12D</sup>* mutation and *Tif1 $\gamma$*  inactivation to induce the formation of IPMNs is still unknown. TAK1 (TGF $\beta$  Associated Kinase 1), which has recently

been proposed to explain R-Ras and TGF $\beta$  cooperation in breast tumors, is an interesting candidate [36].

The relationship between *TIF1 $\gamma$*  and *SMAD4* and their respective role in TGF $\beta$  signaling have been a subject of extensive investigation and debate in the last few years [37]. Indeed, published data support distinct models whereby *TIF1 $\gamma$*  could function as either a negative regulator of TGF $\beta$  signaling [29,30] or a complementary agonist of TGF $\beta$  signaling [32]. In the “antagonist model”, *TIF1 $\gamma$*  negative function relies on its ability to mono-ubiquitinate and relocate *SMAD4* into the cytoplasm. In the “agonist model”, *TIF1 $\gamma$*  competes with *SMAD4* for binding to *SMAD2* and *3* and form *TIF1 $\gamma$ -SMAD2/3* complexes regulating *SMAD4*-independent TGF $\beta$  responses. One can envision that these models, both supported by compelling biochemical and *in vivo* evidence, are not mutually exclusive and that one of them may be predominant depending on the cellular context. The experimental evidence we present here suggest that *TIF1 $\gamma$*  works with *SMAD4* as a complementary agonist molecule during pancreatic tumorigenesis. In the presence of activated *Kras*, *Tif1 $\gamma$*  loss-of-function induces cystic lesions resembling those observed in the absence of *Smad4* suggesting that both molecules act in concert to prevent tumor progression. Even if this hypothesis needs further demonstration, it is strengthened by the observation that *TIF1 $\gamma$*  expression is decreased in human pancreatic tumors and our observation that loss of *Tif1 $\gamma$*  does not significantly impair *Smad4* expression level or *Smad4* target genes expression (data not shown). The existence of a joint effort between *TIF1 $\gamma$*  and *SMAD4* to maintain TGF $\beta$ -mediated tissue homeostasis has been proposed before. Indeed, during erythroid differentiation, *TIF1 $\gamma$*  mediates the differentiation response while *SMAD4* mediates the antiproliferative response [32]. In a recent work, we showed that *Tif1 $\gamma$*  controlled iNKT (invariant Natural Killer T) cell expansion whereas *Smad4* maintained their maturation state [33]. A recent comprehensive genetic analysis of >20,000 transcripts in 24 pancreatic cancers failed to identify point mutations, amplifications, deletion or translocations in the *TIF1 $\gamma$*  gene [20]. The present study strongly spurs us toward looking for *TIF1 $\gamma$*  genetic alterations in a larger set of pancreatic tumors. Besides, chromosomal breakpoints chromosome on 1p13.1 containing *TIF1 $\gamma$*  gene have been reported in acute megakaryocytic leukemias [38], osteochondromas [39], bronchial large cell carcinomas [40] and childhood papillary thyroid carcinomas [41]. Interestingly, we recently demonstrated that abrogation of the closely related *Tif1 $\alpha$*  gene in mice caused hepatocellular carcinoma [42]. These observations reinforce the idea according to which *TIF1 $\gamma$*  loss of function could play an active protective role during tumorigenesis. *TIF1 $\gamma$*  overexpression has been suggested by others to facilitate tumorigenesis in other organs by inhibiting *SMAD4*-mediated growth inhibition and motility in response to TGF $\beta$  [29,30]. This observation may reflect an active role of *TIF1 $\gamma$*  during tumor progression depending on the organ and involving a anti-*SMAD4* mechanisms (“antagonist” model).

In conclusion, we demonstrated in a mouse model that inactivation of *Tif1 $\gamma$*  cooperates with activated *Kras<sup>G12D</sup>* to induce cystic pancreatic tumors. Characterization of new players involved in the outbreak of early pancreatic lesions that will eventually evolve into invasive pancreatic cancer is crucial to detect the disease earlier and eventually develop new therapeutic drugs. Further work to decipher the respective roles of *SMAD4* and *TIF1 $\gamma$*  in PDAC as well as the functional cooperation between *KRAS* and *TIF1 $\gamma$*  could bring new insight into the etiology of pancreatic cancer, and generate a better understanding of the multifaceted role of TGF $\beta$  in carcinogenesis and development.



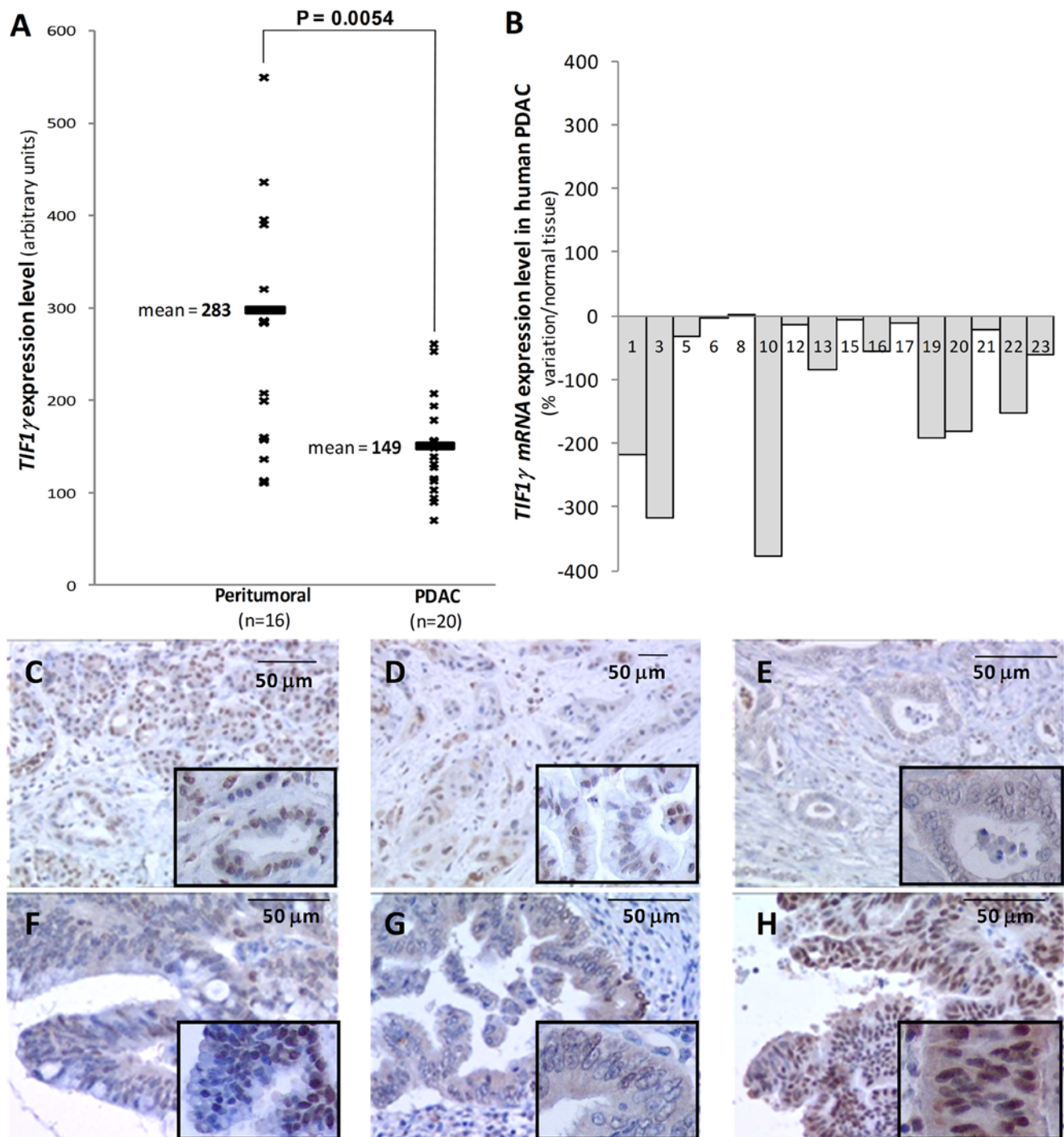


**Figure 5. *TIF1 $\gamma$*  expression in human pancreatic neoplasia.** The expression of *TIF1 $\gamma$*  from 20 human PDAC and 16 peritumoral tissues was determined by quantitative RT-PCR (A). The average expression ( $\pm$ sd) is plotted for each group (B). The significance (P value) for the difference between peritumoral and tumoral groups, determined by a Student's T test, is shown above the graphs. The expression of *TIF1 $\gamma$*  protein was evaluated by immunohistochemistry in different pancreatic lesions: PDAC (n patients=20) (peritumoral (C) and tumoral tissues (D, E). IPMN (n patients=10) of high grade dysplasia (F), high-grade PanINs (n patients=8) (G) and MCN (n patients=15) (H). Inset pictures: higher magnification. doi:10.1371/journal.pgen.1000575.g005

## Materials and Methods

### Mice

*Tif1 $\gamma$ <sup>lox/lox</sup>* [32] mice harboring floxed exons 2–4 were generated by K.Y. and R.L. will be described elsewhere. Briefly, using a genomic clone that contains a portion of the *Tif1 $\gamma$*  gene, we

generated a targeting vector in which a *PGK-Neo* selection cassette flanked by two *loxP* sites was introduced into intron 1 and a third *loxP* site inserted into intron 4. This targeting vector was designed with the expectation that upon homologous recombination and subsequent Cre recombinase-mediated excision, exons 2, 3 and 4 along with the *PGK-Neo* cassette would be deleted, thereby causing



a frameshift mutation with a premature termination codon in exon 5. The putative product of this deleted gene corresponds to a truncated protein lacking part of the RING finger-B box-coiled coil (RBCC) motif and the entire C-terminal region of the TIF1 $\gamma$  protein, which contains the conserved PHD finger/bromodomain unit.

*Ink4A/Arf<sup>lox/lox</sup>* [12], *LSL-Kras<sup>G12D</sup>* [8,43–45] and *Pdx1-Cre* [34] mouse strains done by others were previously described. Mice were maintained in a specific pathogen-free animal facility at the “Centre Léon Bérard” (Lyon, France) and handled in compliance with the institutional guidelines. All procedures were approved by an ethic committee under regulatory of governmental authority (CREEA).

## Histology

Histology experiments were performed as previously described [46]. Primary antibody used were : TIF1 $\gamma$  (1/800; Euromedex), Chymotrypsin (1/1000; AbD Serotec), Insulin (1/1000; Dako), CK19 (1/10; Trauma III - Developmental Studies Hybridoma Bank - University of Iowa), SMAD4 (1/100; Santa Cruz). Alcian blue staining was performed as previously described [47].

## Human samples

Cryopreserved tumoral and peritumoral tissue samples were obtained from an institutional tissue bank, the Tumorothèque des Hospices Civils de Lyon (Centre de Ressources Biologiques, Hospices Civils de Lyon). In accordance with French ethical rules, samples were from patients having given their informed consent or from deceased patients. Prior to molecular analysis, the quality and cellularity of tissue samples was verified histologically; tumor tissues were selected in order to contain a significant amount of neoplastic cells; peritumoral tissues were constantly altered by reactive fibrotic changes associated with a loss in acinar tissue and a massive ductular proliferation.

## RNA analysis

Liquid nitrogen frozen human tumors were blended using a Pro200 homogenizer (Pro Scientific Inc.) in a 5 M guanidine solution. Total RNA was further purified by RNeasy mini kit (Qiagen). The cDNA was used as template with RT Kit SuperScript II (Invitrogen). quantitative RT-PCR was performed as previously described [48].

## Live imaging

For MRI and PET experiments, mice were anesthetized using 3% isoflurane inhalation (TEM Segla, Lormont, France) and maintained in 1.5% isoflurane atmosphere during experiments.

For PET experiments, the mice were catheterized in the caudal vein (24 gauge), injected with 250  $\mu$ Ci of 300  $\mu$ L of radioactive 18-Fluorodéoxyglucose (FDG). After 90 minutes to allow FDG fixation, images were acquired during 15 minutes (constant 2% isoflurane atmosphere) using the “TEP clearPET” (Raytest, Inc.). MRI acquisitions were made with a BioSpec-7T system (Bruker, Ettlingen, Germany) using a 32 mm inner-diameter emission/reception volume coil (Rapid Biomedical, Würzburg, Germany). T1/T2-weighted contrast sequences synchronized to respiration were acquired for each mouse. A RARE (Rapid Acquisition with Relaxation Enhancement) sequence (TR/TE 3500/38.1 ms) with fat saturation was used. Geometric parameters were: a series of 18, 750  $\mu$ m thick sections, 33 mm field of view, and 256 $\times$ 256 pixel matrix. Voxel size was therefore 129 $\times$ 129 $\times$ 750  $\mu$ m<sup>3</sup>.

## Supporting Information

**Figure S1** Loss of nuclear Tif1 $\gamma$  protein expression in the pancreas of *Pdx1-Cre; Tif1 $\gamma$ <sup>lox/lox</sup>* mice. Immunohistochemistry showed that Tif1 $\gamma$  was expressed in the nuclei of pancreatic cells in wild-type mice and that this staining was lost in a *Pdx1-Cre;Tif1 $\gamma$ <sup>lox/lox</sup>* pancreas.

Found at: doi:10.1371/journal.pgen.1000575.s001 (2.25 MB TIF)

**Figure S2** Image of a polycystic pancreas from a 154-day-old *Pdx1-Cre; LSL-Kras<sup>G12D</sup>; Tif1 $\gamma$ <sup>lox/lox</sup>* mouse. Pancreas is circled in black. Note the presence of numerous translucent cysts (arrow-head).

Found at: doi:10.1371/journal.pgen.1000575.s002 (2.96 MB TIF)

**Figure S3** Presence of inflammatory cells in the pancreas associated with the cystic structures. Immunohistochemistry revealed the presence of different populations of leucocytes infiltrating the pancreas of a 20-day-old *Pdx1-Cre; LSL-Kras<sup>G12D</sup>; Tif1 $\gamma$ <sup>lox/lox</sup>* mouse (D–F) compared to a wild-type littermate (A–C). MPO (A,D), F4/80 (B,E), and CD3 (C,F) were respectively used as specific markers for neutrophils, macrophages and lymphocytes. Found at: doi:10.1371/journal.pgen.1000575.s003 (2.71 MB TIF)

**Figure S4** SMAD4 expression in human pancreatic neoplasia. Quantitative RT–PCR to detect SMAD4 expression from the 16 PDAC for which peritumoral tissue was available (A). For each patient represented by an individual bar, SMAD4 expression is represented as a percentage of variation relative to mRNA expression in the peritumoral tissue from the same patient (B). SMAD4 protein expression pattern was also assessed by immunohistochemistry. In the normal pancreas (C), SMAD4 is strongly detected in endocrine islets, a faint labeling is visible in acinar cells and ductal cells. In adenocarcinomas (n patients = 20), no labeling for SMAD4 was detected whereas adjacent residual endocrine cells are positive (D). In another example of adenocarcinoma, SMAD4 is faintly but readily detectable in neoplastic cells; the labeling is both cytoplasmic and nuclear (E). In IPMN grade 3, SMAD4 expression is heterogeneous; most cells are negative, while a few scattered cells retain a faint expression, usually nuclear (F). In PanIN grade 3, SMAD4 expression is either undetectable, as exemplified in the largest figure (note the persistent expression in adjacent residual endocrine cells (arrow)), or heterogeneous, as shown in the inset (G). In MCN, SMAD4 expression is usually strong, in low grade (large figure) as well as in high grade (inset) lesions (H).

Found at: doi:10.1371/journal.pgen.1000575.s004 (3.34 MB TIF)

**Table S1** Measurement of the area occupied by the normal pancreatic tissue.

Found at: doi:10.1371/journal.pgen.1000575.s005 (0.06 MB DOC)

## Acknowledgments

We thank G. Gouysse, J.B. Langlois, S. Martin, M. Janier, P. Meeus, and M. Peix for their expert assistance. We are deeply grateful to D. Wotton for advice, helpful discussions, and proofreading of the manuscript. We thank T. Jacks/R. DePinho, D. Tuveson, and D. Melton for providing *Ink4A/Arf<sup>lox/lox</sup>*, *LSL-Kras<sup>G12D</sup>*, and *Pdx1-Cre* mouse strains.

## Author Contributions

Conceived and designed the experiments: D.F.V. S.M. L.B. Performed the experiments: D.F.V. K.P.Y. I.T. F.G. V.A. B.K. F.L. S.M. S.G.L. S.G. J.Y.S. R.L. L.B. Analyzed the data: D.F.V. I.T. V.A. B.K. J.C.M. S.M. J.L.I. P.D. S.G. A.P. R.R. N.B. J.Y.S. R.L. L.B. Contributed reagents/materials/analysis tools: D.F.V. K.P.Y. I.T. V.A. J.C.M. N.B. J.Y.S. R.L. L.B. Wrote the paper: R.L. L.B.

## References

- Maitra A, Hruban RH (2008) Pancreatic cancer. *Annu Rev Pathol* 3: 157–188.
- Maitra A, Fukushima N, Takaori K, Hruban RH (2005) Precursors to invasive pancreatic cancer. *Adv Anat Pathol* 12: 81–91.
- Furukawa T, Kloppel G, Volkan Adsay N, Albores-Saavedra J, Fukushima N, et al. (2005) Classification of types of intraductal papillary-mucinous neoplasm of the pancreas: a consensus study. *Virchows Arch* 447: 794–799.
- Koorstra JB, Hustinx SR, Offerhaus GJ, Maitra A (2008) Pancreatic carcinogenesis. *Pancreatol* 8: 110–125.
- Bardeesy N, DePinho RA (2002) Pancreatic cancer biology and genetics. *Nature Reviews Cancer* 2: 897–909.
- Shi C, Hruban RH, Klein AP (2009) Familial pancreatic cancer. *Arch Pathol Lab Med* 133: 365–374.
- Hruban RH, Adsay NV, Albores-Saavedra J, Anver MR, Biankin AV, et al. (2006) Pathology of genetically engineered mouse models of pancreatic exocrine cancer: consensus report and recommendations. *Cancer Res* 66: 95–106.
- Hingorani SR, Petricoin EF, Maitra A, Rajapakse V, King C, et al. (2003) Preinvasive and invasive ductal pancreatic cancer and its early detection in the mouse. *Cancer Cell* 4: 437–450.
- Guerra C, Schuhmacher AJ, Canamero M, Grippo PJ, Verdager L, et al. (2007) Chronic pancreatitis is essential for induction of pancreatic ductal adenocarcinoma by K-Ras oncogenes in adult mice. *Cancer Cell* 11: 291–302.
- Grippo PJ, Nowlin PS, Demeure MJ, Longnecker DS, Sandgren EP (2003) Preinvasive pancreatic neoplasia of ductal phenotype induced by acinar cell targeting of mutant Kras in transgenic mice. *Cancer Research* 63: 2016–2019.
- Hingorani SR, Wang L, Multani AS, Combs C, Dermaudt TB, et al. (2005) Trp53R172H and KrasG12D cooperate to promote chromosomal instability and widely metastatic pancreatic ductal adenocarcinoma in mice. *Cancer Cell* 7: 469–483.
- Aguirre AJ, Bardeesy N, Sinha M, Lopez L, Tuveson DA, et al. (2003) Activated Kras and Ink4a/Arf deficiency cooperate to produce metastatic pancreatic ductal adenocarcinoma. *Genes & Development* 17: 3112–3126.
- Bardeesy N, Aguirre AJ, Chu GC, Cheng KH, Lopez LV, et al. (2006) Both p16(Ink4a) and the p19(Arf)-p53 pathway constrain progression of pancreatic adenocarcinoma in the mouse. *Proc Natl Acad Sci U S A* 103: 5947–5952.
- Ijichi H, Chytil A, Gorska AE, Aakre ME, Fujitani Y, et al. (2006) Aggressive pancreatic ductal adenocarcinoma in mice caused by pancreas-specific blockade of transforming growth factor-beta signaling in cooperation with active Kras expression. *Genes Dev* 20: 3147–3160.
- Hezel AF, Gurumurthy S, Granot Z, Swisa A, Chu GC, et al. (2008) Pancreatic LKB1 deletion leads to acinar polarity defects and cystic neoplasms. *Mol Cell Biol* 28: 2414–2425.
- Siveke JT, Einwachter H, Sipos B, Lubeseder-Martellato C, Kloppel G, et al. (2007) Concomitant pancreatic activation of Kras(G12D) and Tgfa results in cystic papillary neoplasms reminiscent of human IPMN. *Cancer Cell* 12: 266–279.
- De La OJ-P, Emerson LL, Goodman JL, Froebe SC, Illum BE, et al. (2008) Notch and Kras reprogram pancreatic acinar cells to ductal intraepithelial neoplasia. *Proc Natl Acad Sci U S A* 105: 18907–18912. Epub 12008 Nov 18921.
- Nolan-Stevaux O, Lau J, Truitt ML, Chu GC, Hebrok M, et al. (2009) GLI1 is regulated through Smoothened-independent mechanisms in neoplastic pancreatic ducts and mediates PDAC cell survival and transformation. *Genes Dev* 23: 24–36.
- Shi G, Zhu L, Sun Y, Bettencourt R, Damsz B, et al. (2009) Loss of the Acinar-Restricted Transcription Factor Mist1 Accelerates Kras-Induced Pancreatic Intraepithelial Neoplasia. *Gastroenterology* 136(4): 1368–1378.
- Jones S, Zhang X, Parsons DW, Lin JC, Leary RJ, et al. (2008) Core signaling pathways in human pancreatic cancers revealed by global genomic analyses. *Science* 321: 1801–1806.
- Bardeesy N, Cheng KH, Berger JH, Chu GC, Pahler J, et al. (2006) Smad4 is dispensable for normal pancreas development yet critical in progression and tumor biology of pancreas cancer. *Genes Dev* 20: 3130–3146.
- Izeradjene K, Combs C, Best M, Gopinathan A, Wagner A, et al. (2007) Kras(G12D) and Smad4/Dpc4 haploinsufficiency cooperate to induce mucinous cystic neoplasms and invasive adenocarcinoma of the pancreas. *Cancer Cell* 11: 229–243.
- Kojima K, Vickers SM, Adsay NV, Jhala NC, Kim HG, et al. (2007) Inactivation of Smad4 accelerates Kras(G12D)-mediated pancreatic neoplasia. *Cancer Res* 67: 8121–8130.
- Kuang C, Xiao Y, Liu X, Stringfield TM, Zhang S, et al. (2006) In vivo disruption of TGF-beta signaling by Smad7 leads to premalignant ductal lesions in the pancreas. *Proc Natl Acad Sci U S A* 103: 1858–1863.
- Ross S, Hill CS (2008) How the Smads regulate transcription. *Int J Biochem Cell Biol* 40: 383–408.
- Massague J, Gomis RR (2006) The logic of TGFbeta signaling. *FEBS Lett* 580: 2811–2820.
- Venturini L, You J, Stadler M, Galien R, Lallemand V, et al. (1999) TIF1gamma, a novel member of the transcriptional intermediary factor 1 family. *Oncogene* 18: 1209–1217.
- Yan KP, Dolle P, Mark M, Lerouge T, Wendling O, et al. (2004) Molecular cloning, genomic structure, and expression analysis of the mouse transcriptional intermediary factor 1 gamma gene. *Gene* 334: 3–13.
- Dupont S, Zacchigna L, Cordenonsi M, Soligo S, Adorno M, et al. (2005) Germ-layer specification and control of cell growth by Ectoderm, a Smad4 ubiquitin ligase. *Cell* 121: 87–99.
- Dupont S, Mamidi A, Cordenonsi M, Montagner M, Zacchigna L, et al. (2009) FAM/USP9x, a deubiquitinating enzyme essential for TGFbeta signaling, controls Smad4 monoubiquitination. *Cell* 136: 123–135.
- Levy L, Howell M, Das D, Harkin S, Episkopou V, et al. (2007) Arkadia activates Smad3/Smad4-dependent transcription by triggering signal-induced SnoN degradation. *Mol Cell Biol* 27: 6068–6083.
- He W, Dorn DC, Erdjument-Bromage H, Tempst P, Moore MA, et al. (2006) Hematopoiesis controlled by distinct TIF1gamma and Smad4 branches of the TGFbeta pathway. *Cell* 125: 929–941.
- Doisne JM, Bartholin L, Yan KP, Garcia CN, Duarte N, et al. (2009) iNKT cell development is orchestrated by different branches of TGF-beta signaling. *J Exp Med* 206: 1365–1378.
- Gu G, Dubauskaite J, Melton DA (2002) Direct evidence for the pancreatic lineage: NGN3+ cells are islet progenitors and are distinct from duct progenitors. *Development* 129: 2447–2457.
- Jorgensen MC, Ahnfelt-Ronne J, Hald J, Madsen OD, Serup P, et al. (2007) An illustrated review of early pancreas development in the mouse. *Endocr Rev* 28: 685–705.
- Erdogan M, Pozzi A, Bhowmick N, Moses HL, Zent R (2008) Transforming growth factor-beta (TGF-beta) and TGF-beta-associated kinase 1 are required for R-Ras-mediated transformation of mammary epithelial cells. *Cancer Res* 68: 6224–6231.
- Heldin CH, Moustakas A (2006) A new twist in Smad signaling. *Dev Cell* 10: 685–686.
- Ng YY, Fan JM, Mu W, Nikolic-Paterson DJ, Yang WC, et al. (1999) Glomerular epithelial-myofibroblast transdifferentiation in the evolution of glomerular crescent formation. *Nephrol Dial Transplant* 14: 2860–2872.
- Sawyer JR, Thomas EL, Lukacs JL, Swanson CM, Ding Y, et al. (2002) Recurring breakpoints of p13 approximately p22 in osteochondroma. *Cancer Genet Cytogenet* 138: 102–106.
- Johansson M, Dietrich C, Mandahl N, Hambræus G, Johansson L, et al. (1994) Karyotypic characterization of bronchial large cell carcinomas. *Int J Cancer* 57: 463–467.
- Klugbauer S, Rabes HM (1999) The transcription coactivator HTIF1 and a related protein are fused to the RET receptor tyrosine kinase in childhood papillary thyroid carcinomas. *Oncogene* 18: 4388–4393.
- Khetchooumian K, Teletin M, Tisserand J, Mark M, Herquel B, et al. (2007) Loss of Trim24 (Tif1alpha) gene function confers oncogenic activity to retinoic acid receptor alpha. *Nat Genet* 39: 1500–1506.
- Jackson EL, Willis N, Mercer K, Bronson RT, Crowley D, et al. (2001) Analysis of lung tumor initiation and progression using conditional expression of oncogenic K-ras. *Genes & Development* 15: 3243–3248.
- Johnson L, Mercer K, Greenbaum D, Bronson RT, Crowley D, et al. (2001) Somatic activation of the K-ras oncogene causes early onset lung cancer in mice. [see comment]. *Nature* 410: 1111–1116.
- Tuveson DA, Shaw AT, Willis NA, Silver DP, Jackson EL, et al. (2004) Endogenous oncogenic K-ras(G12D) stimulates proliferation and widespread neoplastic and developmental defects. *Cancer Cell* 5: 375–387.
- Treilleux I, Blay JY, Bendriss-Vermare N, Ray-Coquard I, Bachelot T, et al. (2004) Dendritic cell infiltration and prognosis of early stage breast cancer. *Clin Cancer Res* 10: 7466–7474.
- Albores-Saavedra J, Weimersheimer-Sandoval M, Chable-Montero F, Montante-Montes de Oca D, Hruban RH, et al. (2008) The foamy variant of pancreatic intraepithelial neoplasia. *Ann Diagn Pathol* 12: 252–259.
- Bartholin L, Cyprian FS, Vincent D, Garcia CN, Martel S, et al. (2008) Generation of mice with conditionally activated transforming growth factor beta signaling through the TbetaRI/ALK5 receptor. *Genesis* 46(12): 724–731.